Self-Consistency versus "Best-Fit" Approaches in Understanding the Structure of Metal Nitrosyl Complexes

David Balcells,[†,‡] Jorge J. Carbó,[†] Feliu Maseras,*[,†,‡] and Odile Eisenstein[§]

Institute of Chemical Research of Catalonia (ICIQ), 43007 Tarragona, Catalonia, Spain, Unitat de Química Física, Edifici Cn, Universitat Autònoma de Barcelona, 08193 Bellaterra, Catalonia, Spain, and LSDSMS (UMR 5636), Université de Montpellier 2, 34095, Montpellier Cedex 5, France

Received June 25, 2004

The metal nitrosyl complexes $RuX(CO)(NO)L_2^+$ ($L = P(^tBu)_2Me$, $X = F^-$, Cl^-, BF_4^-, H_2O, NCH, H^-, no ligand, and CO) have been characterized by computing their structures, relative stabilities, and vibrational frequencies through Becke3LYP calculations on a $RuX(CO)(NO)(PH_3)_2^+$ model complex. In the case of $X = F^-$, Cl^-, BF_4^-, and H_2O, a square pyramidal (SP) geometry with a bent nitrosyl ligand is preferred. In the case of X = NCH, H^-, and CO two geometries exist as local minima: a trigonal bipyramid (TBP) with a linear nitrosyl ligand and a square pyramid with a bent nitrosyl ligand. The computed relative stabilities of such complexes cannot clearly identify the ruthenium coordination geometry. Nevertheless, the correlation between the experimental and theoretical ν_{NO} stretching frequencies is conclusive in identifying $Ru(H)(CO)(NO)L_2$ and $Ru(CO)_2(NO)L_2^+$ as TBP structures and $Ru(NCMe)(CO)(NO)L_2^+$ as SP. Three sets of additional calculations were also carried out on a selected system ($X = H^-$). The computational level was increased to CCSD(T), the solvent effect was introduced with a PCM approach, and the real phosphine ligands were considered with a QM/MM ONIOM method.

1. Introduction

Metal nitrosyls are of great current interest.[1−3] Although CO and NO^+ ligands are isoelectronic, their chemistry is completely different due to the much higher electron-withdrawing character of NO. Many experimental[4−9] and theoretical[9−16] studies showed the unique structural and chemical properties of metal nitrosyls. Especially significant are the two possible coordination modes of NO, linear (NO^+) and bent (NO^-).[17−20] The change in the formal charge of NO changes the formal oxidation state of the metal and therefore also the coordination geometry. It is important to have an understanding of the preferred coordination modes of the nitrosyl ligand because of its reactivity. The NO molecule is activated by coordination and reacts with Lewis acids[21,22] and protons[23,24] or with N−O bond cleavage;[25,26] it also has important biological activities.[27−34] Moreover, metal nitrosyls have been proposed

[†] ICIQ.
[‡] Universitat Autònoma de Barcelona.
[§] Université de Montpellier 2.

(1) Richter-Addo, G. B.; Legzdins, P. *Metal Nitrosyls*; Oxford University Press: New York, 1992.
(2) Hayton, T. W.; Legzdins, P.; Sharp, W. B. *Chem. Rev.* **2002**, *102*, 935.
(3) Ford, P. C.; Lorkovic, I. M. *Chem. Rev.* **2002**, *102*, 993.
(4) Daff, P. J.; Legzdins, P.; Rettig, S. J. *J. Am. Chem. Soc.* **1998**, *120*, 2688.
(5) Smith, K.; McNeil, W.; Legzdins, P. *Chem. Eur. J.* **2000**, *6*, 1525.
(6) Matsukawa, S.; Kuwata, S.; Hidai, M. *Inorg. Chem.* **2000**, *39*, 791.
(7) Llamazares, A.; Schmalle, H. W.; Berke, H. *Organometallics* **2001**, *20*, 5277.
(8) Renkema, K.; Caulton, K. G. *New J. Chem.* **1999**, *23*, 1027.
(9) Huang, D.; Streib, W. E.; Eisenstein, O.; Caulton, K. G. *Organometallics* **2000**, *19*, 1967.
(10) Niu, S.; Hall, M. B. *J. Am. Chem. Soc.* **1997**, *119*, 3077.
(11) Hu, C. H.; Chong, D. P. *Chem. Phys. Lett.* **1996**, *262*, 733.
(12) Blanchet, C.; Duarte, H. A.; Salahub, D. R. *J. Chem. Phys.* **1997**, *106*, 8778.
(13) Thomas, J. L.; Bauschlicher, C. W.; Hall, M. B. *J. Phys. Chem. A* **1997**, *101*, 8530.
(14) Ara, I.; Fornies, J.; Garcia-Monforte, M.; Menjon, B.; Sanz-Carrillo, R. M.; Tomas, M.; Tsipis, A. C.; Tsipis, C. A. *Chem. Eur. J.* **2003**, *9*, 4094.
(15) Wang, H. F.; Miki, E.; Re, S. Y.; Tokiwa, H. *Inorg. Chim. Acta* **2002**, *340*, 119.
(16) Andrews, L.; Citra, A. *Chem. Rev.* **2002**, *102*, 885.
(17) Coppens, P.; Fomitchev, D. V.; Carducci, M. D.; Culp, K. *J. Chem. Soc., Dalton Trans.* **1998**, 865.
(18) Basolo, F. *Polyhedron* **1990**, *9*, 1503.
(19) Rizopoulos, A. L.; Sigalas, M. *New J. Chem.* **2001**, *25*, 981.
(20) Coppens, P.; Novozhilova, I.; Kovalevsky, A. *Chem. Rev.* **2002**, *102*, 861.
(21) Sharp, W. B.; Legzdins, P.; Patrick, B. O. *J. Am. Chem. Soc.* **2001**, *123*, 8143.
(22) Bohmer, J.; Haselhorst, G.; Wieghardt, K.; Nuber, B. *Angew. Chem., Int. Ed. Engl.* **1994**, *33*, 1473.
(23) Hash, K. R.; Rosenberg, E. *Organometallics* **1997**, *16*, 3593.
(24) Sellmann, D.; Gottschalk-Gaudig, T.; Haussinger, D.; Heinemann, F. W.; Hess, B. A. *Chem. Eur. J.* **2001**, *7*, 2099.
(25) Brouwer, E. B.; Legzdins, P.; Rettig, S. J.; Ross, K. J. *Organometallics* **1994**, *13*, 2088.
(26) Veige, A. S.; Slaughter, L. M.; Wolczanski, P. T.; Matsunaga, N.; Decker, S. A.; Cundari, T. R. *J. Am. Chem. Soc.* **2001**, *123*, 6419.
(27) Koshland, D. E. J. *Science* **1992**, *258*, 1861.
(28) Culatta, E.; Koshland, D. E. J. *Science* **1992**, *258*, 1862.
(29) Jia, L.; Bonaventura, C.; Bonaventura, J.; Stamler, J. S. *Nature* **1996**, *380*, 221.
(30) Wang, P. G.; Xian, M.; Tang, X.; Wu, X.; Wen, Z.; Cai, T.; Janczuk, A. J. *Chem. Rev.* **2002**, *102*, 1091.
(31) Butler, A. R.; Megson, I. L. *Chem. Rev.* **2002**, *102*, 1155.
(32) Moller, J. K. S.; Skibsted, L. H. *Chem. Rev.* **2002**, *102*, 1167.
(33) Wasser, I. M.; Vries, de S.; Moënne-Loccoz, P.; Schröder, I.; Karlin, K. D. *Chem. Rev.* **2002**, *102*, 1201.

10.1021/om049536+ CCC: $27.50
Publication on Web 11/03/2004

as intermediates in the catalyzed NO disproportionation[35,36] and NO reduction.[37,38]

The entire family of metal nitrosyl ruthenium complexes $RuX(CO)(NO)L_2^+$ (X = F^-, Cl^-, BF_4^-, H_2O, NCMe, H^-, no ligand, and CO)[39] protected by the bulky phosphine L = $P(^tBu)_2Me$[40,41] was characterized some years ago. Since the NO can be linear or bent, two electronic states of each complex may exist: d^6 Ru^{II} with bent NO^- and d^8 Ru^0 with linear NO^+. The Ru^{II} state has square pyramidal (SP) coordination geometry, while Ru^0 is trigonal bipyramidal (TBP). These two states may have very close stabilities and coexist in solution, as observed in other ruthenium systems.[42] The full $RuX(CO)(NO)L_2^+$ series was characterized by means of experimental (X-ray diffraction and IR) and theoretical (DFT Becke3LYP calculations; L = PH_3) methods. Nevertheless, the molecular structure was not clearly determined in all cases. Neither the computed potential energies nor the experimental data were enough to precisely determine the coordination geometry of ruthenium in the metal nitrosyls $Ru(NCMe)(CO)(NO)L_2^+$ and $Ru(CO)_2(NO)L_2^+$. We thus decided to carry out a new study to solve this issue.

In this article we present an improved theoretical study on the isomers in this family of ruthenium compounds. The relative potential energies (*E*), enthalpies (*H*), and Gibbs free energies (*G*) are computed, together with their NO and CO stretching vibrational frequencies at the DFT Becke3LYP level. Calculations on a selected system (X = H^-) were performed to evaluate the computational level and the validity of the model. CCSD(T) calculations were carried out. The real phosphines were considered with a QM/MM (ONIOM) approach. The influence of the solvent was tested with a PCM method. The results show that none of the energetical information can decisively discriminate between the two structures. The usual computational solution to this problem would be to increase the quality in the methodological description, as well as in the modelization of the system. Instead, here we follow a different approach, which increases only modestly the computer effort. It is the comparison of experimental and theoretical vibrational stretching frequencies that has previously been used for structural characterization of many compounds.[43−46] We show in what follows that the structures of $RuX(CO)(NO)L_2^+$ (X = NCMe, H^-, and CO) can be conclusively assigned by correlating the experimental and theoretical nitrosyl vibrational frequencies for the whole $RuX(CO)(NO)L_2^+$ family.

2. Computational Details

The bulk of the results reported in this paper were obtained using the hybrid Becke3LYP density functional[47,48] as implemented within the Gaussian03 package.[49] The 6-31G(d)[50,51] basis set was used for fluorine, oxygen, nitrogen, carbon, and hydrogen. An effective core potential was used to replace the innermost electrons of phosphorus,[52] chlorine,[52] and ruthenium.[53] The valence double-ζ basis set associated with the pseudopotential in the program,[49] with the contraction labeled as LANL2DZ, was used for these two elements and supplemented with a d shell in the case of phosphorus and chlorine.[54] All the geometry optimizations were carried out without imposing constraints. The previously reported theoretical study[39] was improved by the calculation of the enthalpic (*H*) and Gibbs free energies (*G*) together with the vibrational frequencies of all the located energy minima. These frequencies were obtained from the analytical calculation of the second derivatives of the potential energy. The *H* and *G* values reported correspond to a temperature of 25 °C and a pressure of 1 atm. The bulky phosphines and the NCMe ligand were modeled as PH_3 and NCH, respectively.

An additional set of more accurate calculations were carried out on one of the systems. More accurate energies were obtained with the CCSD(T) method,[55,56] solvent effects were introduced with the PCM approach,[57,58] and the real phosphine substituents were considered with the ONIOM method.[59,60]

3. Results and Discussion

3.1. Structures and Energies. All the possible minimum energy structures of $RuX(CO)(NO)L_2^+$ were located in the corresponding potential energy surfaces (PES) for X = F^- (**1**), Cl^- (**2**), BF_4^- (**3**), H_2O (**4**), no ligand (**5**), NCH (**6**, **7**), H^- (**8**, **9**), and CO (**10**, **11**). The

(34) Nagano, T.; Yoshimura, T. *Chem. Rev.* **2002**, *102*, 1235.
(35) Franz, K. J.; Lippard, S. J. *J. Am. Chem. Soc.* **1998**, *120*, 9034.
(36) Franz, K. J.; Lippard, S. J. *J. Am. Chem. Soc.* **1999**, *121*, 10504.
(37) Wang, Y.; Dasilva, J.; Pombeiro, A. J. L.; Pellinghelli, M. A.; Tiripicchio, A. *J. Organomet. Chem.* **1994**, *476*, C9.
(38) MacNeil, J. H.; Gantzel, P. K.; Trogler, W. C. *Inorg. Chim. Acta* **1995**, *240*, 299.
(39) Ogasawara, M.; Huang, D.; Streib, W. E.; Huffman, J. C.; Gallego-Planas, N.; Maseras, F.; Eisenstein, O.; Caulton, K. G. *J. Am. Chem. Soc.* **1997**, *119*, 8642.
(40) Ogasawara, M.; Macgregor, S. A.; Streib, W. E.; Folting, K.; Eisenstein, O.; Caulton, K. G. *J. Am. Chem. Soc.* **1995**, *117*, 8869.
(41) Ogasawara, M.; Macgregor, S. A.; Streib, W. E.; Folting, K.; Eisenstein, O.; Caulton, K. G. *J. Am. Chem. Soc.* **1996**, *118*, 10189.
(42) Ogasawara, M.; Maseras, F.; Gallego-Planas, N.; Streib, W. E.; Eisenstein, O.; Caulton, K. G. *Inorg. Chem.* **1996**, *35*, 7468.
(43) Vázquez, J.; González, J. J. L.; Márquez, F.; Pongor, G.; Boggs, J. E. *J. Phys. Chem. A* **2000**, *104*, 2599.
(44) Khabashesku, V. N.; Kudin, K. N.; Margrave, J. L. *Russ. Chem. Bull.* **2001**, *50*, 20.
(45) Erben, M. F.; Vedova, C. O. D.; Boese, R.; Willner, H.; Leibold, C.; Oberhammer, H. *Inorg. Chem.* **2003**, *42*, 7297.
(46) Diep, V.; Dannenberg, J. J.; Franck, R. W. *J. Org. Chem.* **2003**, *68*, 7907.
(47) Becke, A. D. *J. Chem. Phys.* **1993**, *98*, 5648.
(48) Lee, C.; Yang, W.; Parr, R. G. *Phys. Rev.* **1988**, *37*, B785.
(49) Frisch, M. J.; Trucks, G. W.; Schlegel, H. B.; Scuseria, G. E.; Robb, M. A.; Cheeseman, J. R.; Montgomery, J. A., Jr.; Vreven, T.; Kudin, K. N.; Burant, J. C.; Millam, J. M.; Iyengar, S. S.; Tomasi, J.; Barone, V.; Mennucci, B.; Cossi, M.; Scalmani, G.; Rega, N.; Petersson, G. A.; Nakatsuji, H.; Hada, M.; Ehara, M.; Toyota, K.; Fukuda, R.; Hasegawa, J.; Ishida, M.; Nakajima, T.; Honda, Y.; Kitao, O.; Nakai, H.; Klene, M.; Li, X.; Knox, J. E.; Hratchian, H. P.; Cross, J. B.; Adamo, C.; Jaramillo, J.; Gomperts, R.; Stratmann, R. E.; Yazyev, O.; Austin, A. J.; Cammi, R.; Pomelli, C.; Ochterski, J. W.; Ayala, P. Y.; Morokuma, K.; Voth, G. A.; Salvador, P.; Dannenberg, J. J.; Zakrzewski, V. G.; Dapprich, S.; Daniels, A. D.; Strain, M. C.; Farkas, O.; Malick, D. K.; Rabuck, A. D.; Raghavachari, K.; Foresman, J. B.; Ortiz, J. V.; Cui, Q.; Baboul, A. G.; Clifford, S.; Cioslowski, J.; Stefanov, B. B.; Liu, G.; Liashenko, A.; Piskorz, P.; Komaromi, I.; Martin, R. L.; Fox, D. J.; Keith, T.; Al-Laham, M. A.; Peng, C. Y.; Nanayakkara, A.; Challacombe, M.; Gill, P. M. W.; Johnson, B.; Chen, W.; Wong, M. W.; Gonzalez, A.; Pople, J. A. *Gaussian 03*, Revision B.02; Gaussian Inc., Pittsburgh, PA, 2003.
(50) Hehre, W. J.; Ditchfield, R.; Pople, J. A. *J. Phys. Chem.* **1972**, *56*, 2257.
(51) Hariharan, P. C.; Pople, J. A. *Theor. Chim. Acta* **1973**, *28*, 213.
(52) Wadt, W. R.; Hay, P. J. *J. Chem. Phys.* **1985**, *82*, 284.
(53) Hay, P. J.; Wadt, W. R. *J. Chem. Phys.* **1985**, *82*, 299.
(54) Francl, M. M.; Pietro, W. J.; Hehre, W. J.; Binkley, J. S.; Gordon, M. S.; Defrees, D. J.; Pople, J. A. *J. Phys. Chem.* **1982**, *77*, 3654.
(55) Purvis, G. D.; Bartlett, R. J. *J. Chem. Phys.* **1982**, *76*, 1910.
(56) Raghavachari, K.; Trucks, G. W.; Pople, J. A.; Head-Gordon, M. *Chem. Phys. Lett.* **1989**, *147*, 479.
(57) Miertus, S.; Scrocco, E.; Tomasi, J. *Comput. Phys.* **1981**, *55*, 117.
(58) Cossi, M.; Barone, V.; Cammi, R.; Tomasi, J. *Chem. Phys. Lett.* **1996**, *255*, 327.
(59) Maseras, F.; Morokuma, K. *J. Comput. Chem.* **1995**, *16*, 1170.
(60) Vreven, T.; Morokuma, K. *J. Comput. Chem.* **2000**, *21*, 1419.

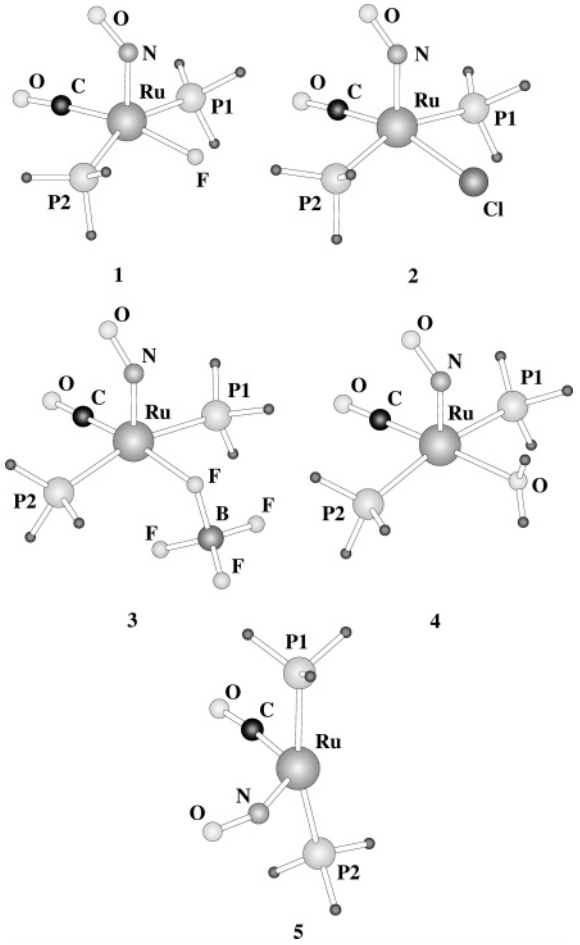

Figure 1. Optimized structures of $RuX(CO)(NO)L_2^+$ (X = F^-, Cl^-, BF_4^-, H_2O, no ligand).

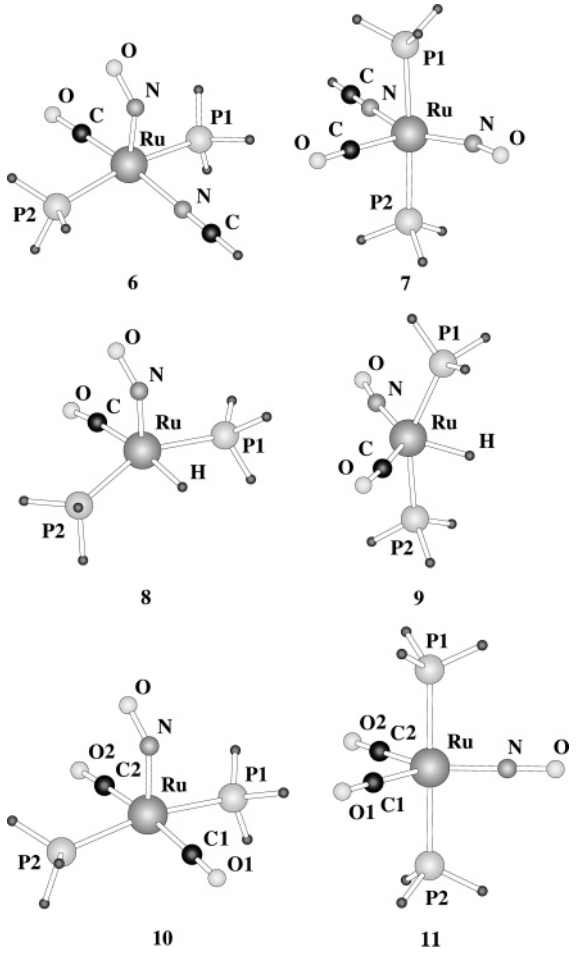

Figure 2. Optimized structures of $RuX(CO)(NO)L_2^+$ (X = NCH, H^-, CO).

structures **1**−**5** and **6**−**11** are represented in Figures 1 and 2, respectively. The structural parameters of the SP and TBP isomers are collected in Tables 1 and 2, respectively.

A SP structure, with a bent NO ligand, was found for **1**−**4**, **6**, **8**, and **10**. The geometry of complex **1** is representative of the structures of the entire group. According to the dihedral angles F−Ru−P1−CO, P1−Ru−C(O)−P2, and OC−Ru−P1−NO of 165.4°, 161.8°, and 96.6°, respectively (see Table 1), the metal nitrosyl **1** has a distorted SP geometry with the NO apical and the CO, PH_3, and F ligands in the square base. The P1−Ru−P2 and F−Ru−CO bond angles of 157.5° and 165.4°, respectively, indicate that the phosphines and the F,CO pair of ligands are each *trans*. Furthermore, the Ru−N−O bond angle of 128.4° clearly indicates a bent NO ligand.

All attempts to optimize the TBP isomers of $RuX(CO)(NO)L_2^+$ failed for X = F^-, Cl^-, BF_4^-, and H_2O. In all cases, the energy minimization algorithm converged on the SP geometries **1**−**4**. This result shows that bent NO is the only favored coordination mode of the nitrosyl ligand when X is a π-donor. In contrast, the TBP structures **5**, **7**, **9**, and **11** were found in the PES of X = no ligand, NCH, H^-, and CO, respectively (see Figure 2). Thus, linear NO associated with the TBP coordination and bent NO associated with the SP geometry are possible when X is a pure σ-donor ligand or is a π-acceptor ligand. It is also the preferred geometry when there is no ligand X.

Table 1. Bond Distances (Å), Bond Angles (deg), and Dihedral Angles (deg) of All SP Isomers of $RuX(CO)(NO)L_2^+$[a]

	X =						
	F^- (**1**)	Cl^- (**2**)	BF_4^- (**3**)	H_2O (**4**)	NCH (**6**)	H^- (**8**)	CO (**10**)
N−O	1.180	1.178	1.181	1.169	1.168	1.179	1.165
C−O	1.161	1.159	1.158	1.151	1.150	1.158	1.143
Ru−N−O	128.4	129.3	128.4	127.7	125.7	129.3	121.8
Ru−C−O	175.9	177.4	179.8	179.5	179.6	173.2	177.8
P1−Ru−P2	157.5	159.6	164.5	166.3	166.4	152.4	165.7
X−Ru−CO	165.4	159.9	170.2	173.4	172.1	166.9	171.9
X−Ru−P1−CO	165.4	160.0	170.3	174.9	172.1	167.0	172.0
P1−Ru−C(O)−P2	161.8	162.2	165.1	166.3	166.5	157.2	165.9
OC−Ru−P1−NO	96.6	97.9	99.0	100.0	97.8	98.7	97.2

[a] In the case of $Ru(CO)_2(NO)L_2^+$, the values given correspond to the CO labeled as C(2)−O(2) in Figure 2.

The TBP geometry of **7** (X = NCH) is clearly indicated by the bond angles P1−Ru−P2, OC−Ru−NO, HCN−Ru−NO, and HCN−Ru−CO of 175.5°, 116.1°, 143.3°, and 100.6°, respectively (see Table 2). The first angle is very close to 180°, indicating that the phosphines are axial, while the other angles, close to 120°, mean that the (NO)(CO)(NCH) set forms the equatorial plane of the TBP structure. The Ru−N−O bond angle of 154.2° in this TBP isomer shows that the NO ligand is closer to being linear than in the SP isomer **6** (125.7°). In the case of X = H^- and CO the linear NO ligand is indicated by Ru−N−O bond angles of 171.5° and 180.0°, respectively. The special case of X = NCH with an open

Table 2. Bond Distances (Å), Bond Angles (deg), and Dihedral Angles (deg) of All TBP Isomers of $RuX(CO)(NO)L_2^+$[a]

	X =			
	no ligand (**5**)	NCH (**7**)	H^- (**9**)	CO (**11**)
N−O	1.158	1.165	1.180	1.157
C−O	1.149	1.151	1.158	1.143
Ru−N−O	147.5	154.2	171.5	180.0
Ru−C−O	172.9	173.9	174.8	177.1
P1−Ru−P2	166.1	175.5	153.7	179.4
OC−Ru−NO	120.1	116.1	133.8	130.3
X−Ru−NO		143.3	133.1	130.4
X−Ru−CO		100.6	93.1	99.3

[a] In the case of $Ru(CO)_2(NO)L_2^+$, the values given correspond to the CO labeled as C(2)−O(2) in Figure 2.

Table 3. Relative Potential, Enthalpic, and Free Gibbs Energies of the SP and TBP Isomers of X = NCH, H^-, and CO[a]

X	E(TBP) − E(SP)	H(TBP) − H(SP)	G(TBP) − G(SP)
NCH (**6**, **7**)	5.16	5.32	4.50
H (**8**, **9**)	−0.03	0.45	0.41
CO (**10**, **11**)	1.15	1.58	0.82

[a] All energies are in kcal/mol. A positive number means that the SP structure is more stable.

Ru−N−O angle significantly larger than the ones traditionally obtained for bent NO but smaller than for a linear NO led to the proposal of a continuum of metal oxidation states.[39]

The relative E, H, and G energies of the complexes **6**−**11** were computed in order to infer the stabilities of each SP and TBP isomer (see Table 3). While there is a slight preference for the SP geometry in the case of X = NCH and CO, the calculations show the SP and TBP isomers have essentially the same values for E, H, and G for $X = H^-$. This should lead to equilibrium in solution at room temperature between the two isomers, which is not suggested by the experimental results. Furthermore the solid state structure for $X = H^-$ shows that the preferred geometry is TBP.

At this point, one can try to improve the quality of the calculation, and there are a variety of ways to do it. We applied several of them to the particular case of $X = H^-$, complexes **8** and **9**. The first improvement was to increase the computational level. DFT in general and Becke3LYP in particular provide good quality results for transition metal complexes, but these are usually inferior in quality to those of the CCSD(T) method, which in contrast is much more demanding in terms of computational resources. We carried out single-point energy calculations at the CCSD(T) level on the Becke3LYP optimized structures of complexes **8** and **9**. The difference in the potential energies, which was 0.03 kcal/mol in favor of TBP (**9**) at the Becke3LYP level, was slightly increased to 0.13 kcal/mol in favor of the same TBP form. The similarity of the results suggests that Becke3LYP is sufficiently accurate for this type of systems, but leaves unexplained the experimental presence of only one isomer. A second improvement was to analyze the influence of the environment. The previous calculations represent species in the vacuum. In contrast, IR measurements are done in solution and X-ray structural information comes from the solid state. The influence of dichloromethane, the solvent used for the IR measurements, was evaluated through single-point PCM calculations on complexes **8** and **9**. In this case, the results were also essentially unchanged: the TBP species is found 0.34 kcal/mol below the SP complex. Again, this fails to explain the presence of only one isomer in the experiment.

The third and last improvement considered was that of the modelization of the phosphine ligands. All the previous calculations used PH_3 as ligands, while experimental data had been obtained with P^tBu_2Me. We introduced the steric effect of the real ligands through ONIOM (Becke3LYP:UFF) geometry optimizations, using the model system defined above as the quantum mechanical region. Several conformations had to be searched to find the most stable one for each coordination mode,[61] and the final result was that the TBP structure is 2.29 kcal/mol more stable than the SP geometry. As expected from the *trans* arrangement of the phosphines, the P−Ru−P bond angle is very similar in both structures, 157.8° for SP and 157.2° for TBP, and direct phosphine−phosphine interactions cannot explain the steric effect of the substituents. Instead the key factor seems to be the steric resulsions between the phosphine substituents and the three ligands in the plane perpendicular to the P−Ru−P axis. The TBP arrangement with L−Ru−L angles around 120° fits better with the C_3-like distribution of phosphine substituents than the T-shape (ideal angles closer to 90° and 180°) associated with the SP arrangement.

The energy difference above 2 kcal/mol between both coordination modes in the ONIOM calculation is certainly sufficient to explain the experimental observation of only one form in the IR measurements. The introduction of the steric effect of the phosphine substituents is thus necessary to obtain an accurate estimation of the relative stability of the TBP and SP isomers. The importance of the steric effects of phosphine substituents on the relative stability of the isomeric forms of ruthenium complexes had in fact already been reported.[42,62]

The systematic use of different computational approaches on the hydride complexes shows therefore that the use of a model closer to the real system can indeed reproduce the experimental observation. This does not alter however the fact that both isomers remain very close in energy and that the reliability of the computational approaches is always questionable when such small differences are involved. Moreover, the need to associate the ONIOM calculation with a conformational search makes its performance more complicated than the straightforward Becke3LYP calculation on the model system with PH_3 substituents. Because of this, it would be desirable to find a method that could assign the nature of the isomer, TBP or SP, directly from the Becke3LYP calculations on the model systems.

From the geometry optimization and energy calculations at the Becke3LYP level on a model system, it appears that (i) the SP geometry and the associated d^6 Ru^{II} electronic state are preferred for π-donor X groups, (ii) the TBP geometry and the associated d^8 Ru^0 electronic state are preferred when X is a σ-donor or a

(61) Balcells, D.; Drudis-Solé, G.; Besora, M.; Dölker, N.; Ujaque, G.; Maseras, F.; Lledós, A. *Faraday Discuss.* **2003**, *124*, 429.
(62) Ogasawara, M.; Maseras, F.; Gallego-Planas, N.; Kawamura, K.; Ito, K.; Toyota, K.; Streib, W. E.; Komiya, S.; Eisenstein, O.; Caulton, K. G. *Organometallics* **1997**, *16*, 1979.

Table 4. NO and CO Frequencies (cm^{-1}) of $RuX(NO)(CO)L_2^+$[a]

X	$\nu_{NO,exp}$	$\nu_{NO,theor}$	$\nu_{CO,exp}$	$\nu_{CO,theor}$
F^-	1568	1752	1912	2054
Cl^-	1570	1763	1914	2061
BF_4^-	1572	1754	1917	2073
H_2O	1607	1808	1950	2114
NCH	1609	1812 (**6**), 1874 (**7**)	1960	2120 (**6**), 2110 (**7**)
H^-	1616	1757 (**8**), 1807 (**9**)	1896	2063 (**8**), 2058 (**9**)
no ligand	1709	1897	1966	2122
CO	1738	1822 (**10**), 1924 (**11**)	1996	2142 (**10**), 2137 (**11**)
			2047	2200 (**10**), 2172 (**11**)

[a] When both SP and TBP isomers are possible, the corresponding structure label is indicated within parentheses. Structures **6**, **8**, and **10** are SP and **7**, **9**, and **11** are TBP.

π-acceptor or when there is no ligand X, and (iii) no reliable structural preference can be deduced from the geometry optimization for X = NCH, H^-, and CO. We would like to show here that in place of carrying out time-consuming calculations we can obtain more reliable information from the calculations of the IR spectra and notably from the NO stretching frequencies.

3.2. IR Spectra. The data presented above confirm that SP/TBP isomerism is directly associated with a change in the NO coordination mode. The SP complexes have a bent NO^-, while the TBP complexes have a linear NO^+. Since the d orbitals of ruthenium are strongly interacting with the π and π^* orbitals of the nitrosyl ligand,[1] the bending of the Ru−N−O bond angle implies a perturbation of the N−O bond. This effect can be appreciated in the case of $Ru(CO)_2(NO)L_2^+$, where a Ru−N−O angle bending of 58.2° (from 180.0° in **11** to 121.8° in **10**) results in a N−O bond elongation of 0.008 Å (from 1.157 Å in **11** to 1.165 Å in **10**). In general, when the two coordination geometries were characterized, the N−O bond distances found in both isomers were only slightly different (see Tables 1 and 2).

The small variations of the N−O bond distances result in a significant variation of ν_{NO} due to the high strength of this bond. This effect was explored through the analytical calculation of the NO stretching frequencies for the full $RuX(CO)(NO)L_2^+$ series of ruthenium nitrosyls (see Table 4). According to our results, as the distortion of the N−O bond distance increases from 0.001 Å (X = H^-) to 0.008 Å (X = CO), the difference between $\nu_{NO,SP}$ and $\nu_{NO,TBP}$ also increases from 50 to 102 cm^{-1}, respectively. The shift of the NO stretching frequencies is clearly observed in the IR spectra and is experimentally well known.[16,39,63,64] In general, bent NO has a lower ν_{NO} than linear NO. This trend is followed by the $RuX(CO)(NO)L_2^+$ nitrosyls since all the complexes with bent NO (X = F^-, Cl^-, BF_4^-, and H_2O) have the lowest experimental and computed NO stretching frequencies (see Table 4). Moreover, the values of ν_{NO} computed for X = NCH, H^-, and CO are in all cases higher for the TBP geometry than for the SP structure. This trend could be in principle used to predict the NO coordination mode and, therefore, the structure of $RuX(CO)(NO)L_2^+$. The stretching NO frequencies should span a different range for a bent or linear ligand. This could be used to assign a structure if the two domains of frequencies have no large overlap. However this is not the case. The $RuH(CO)(NO)L_2$ complex illustrates the difficulties. The experimental ν_{NO} of 1616 cm^{-1} (see Table 4) is very close to the range seen for SP isomers (1568 cm^{-1} (X = F^-), 1570 cm^{-1} (X = Cl^-), 1572 cm^{-1} (X = BF_4^-), and 1607 cm^{-1} (X = H_2O)). Thus, the ν_{NO} for X = H^- seems to be near the low-frequency region of SP-bent-NO^+ complexes. However, the coordination symmetry around ruthenium in this species was fully characterized by X-ray diffraction as TBP. Thus, the experimental ν_{NO} frequencies are unable to predict the coordination geometry.

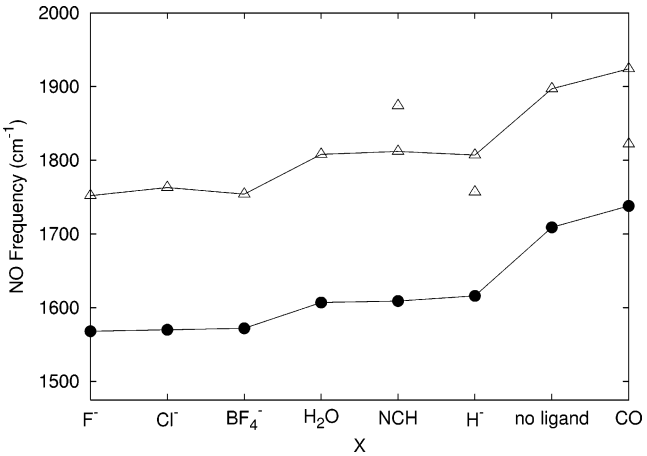

Figure 3. Correlation between experimental (●) and theoretical (△) ν_{NO}.

Direct comparison of experimental and computed values for ν_{NO} is not a conclusive approach either. In this case, $RuH(CO)(NO)L_2$ is again a useful reference. The deviation of $\nu_{NO,theor}$ with respect to $\nu_{NO,exp}$ for this complex is clearly higher for the TBP geometry (191 cm^{-1}) than for the SP (141 cm^{-1}). However, $RuH(CO)(NO)L_2$ was experimentaly characterized as TBP. Thus, neither the experimental ν_{NO} frequencies, nor the theoretical values of ν_{NO}, nor the direct comparison between them can be used to achieve a reliable characterization of $RuX(CO)(NO)L_2^+$ (X = NCH, H^-, and CO).

Trends in the experimental ν_{NO} stretching frequencies are faithfully reproduced by the calculations, suggesting that the correlation can be used for resolving the ambiguous cases. The experimental and calculated values of ν_{NO} stretching frequencies for all $RuX(CO)(NO)L_2^+$ complexes were plotted in Figure 3. In all cases where we see only one calculated minimum for $RuX(CO)(NO)L_2^+$, the calculated frequency is higher than the measured value with a systematic deviation of ca. 200 cm^{-1}, likely due in part to the harmonic approxima-

(63) Wang, H.; Hagihara, T.; Ikezawa, H.; Tomizaea, H.; Miki, E. *Inorg. Chim. Acta* **2000**, *299*, 80.
(64) Vogel, K. M.; Kozlowski, P. M.; Zgierski, M. Z.; Spiro, T. G. *J. Am. Chem. Soc.* **1999**, *121*, 9915.

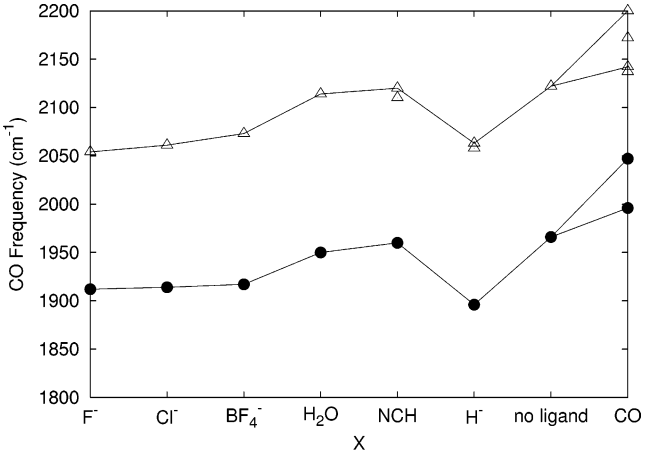

Figure 4. Correlation between experimental (●) and theoretical (△) ν_{CO}.

tion used in the calculations.[65] Because of the constant shift, the patterns for the experimental and calculated frequencies are very similar. For the cases where SP and TBP structures have been found, there are two possible values for the stretching frequencies. Making the reasonable assumption that $RuX(CO)(NO)L_2^+$ is a homogeneous family, the calculated ν_{NO} stretching frequencies should not deviate from the pattern found for the other members of the family. This leads us to a clear identification: the structure with the lower ν_{NO} stretching frequency (SP) for X = NCH and the structure with the higher frequency (TBP) for X = H^- and CO. Strong singularities in the curves would result from selecting the alternative structures. By this method, we select the structure also observed in the solid state for the case of X = H^-. This study thus suggests that the structure is SP for X = NCMe and TBP for X = CO. This method leads to selecting a structure that does not necessarily correspond to the structure having the calculated stretching frequency closest to the experimental value but the one that agrees with the trend within the entire family. The only assumption in this method is that the shift between calculated and experimental frequencies is approximately constant within a homogeneous family.

The CO frequencies (ν_{CO}) of $RuX(CO)(NO)L_2^+$, which are experimentally known, were also computed (see Table 4). While the differences between $\nu_{NO,SP}$ and $\nu_{NO,TBP}$ are within the range 50−102 cm^{-1}, the maximum variation of ν_{CO} is only 28 cm^{-1}. This slight variation of ν_{CO} is due to the minimal distortion of the CO coordination to ruthenium reflected by the small differences of the C−O bond distance and Ru−C−O bond angle between the SP and TBP structures. The largest deviations in these geometric parameters are 0.001 Å and 5.7° for X = NCH (see Tables 1 and 2) and correspond to the highest ν_{CO} variation. The sensitivity of the ν_{CO} stretching frequency to the nature of X and to the coordination at the metal is too small to allow a safe discrimination between the SP and TBP structures. This is clearly illustrated in Figure 4, where the experimental and calculated ν_{CO} stretching frequencies are plotted. The ν_{CO} values corresponding to X = NCH, H^-, and CO are close on this diagram, and the correlation is essentially unaffected by the selection of the SP or the TBP structures for any of these three complexes.

The preference for an SP geometry and a bent nitrosyl ligand has been previously discussed in the earlier work.[39] We focus here on the use of frequencies for determination of structures. First of all, it is well recognized that structure assignment can be obtained from a good agreement between calculated and experimental frequencies. This method has been successfully used by Andrews in particular for assigning the structures of short-lived transition metal complexes including metal carbonyl and nitrosyl complexes.[16] We have applied the same idea of this method for structure determination but with a different point of view.

The ν_{CO} stretching frequencies, often considered as sensitive reporters of the electron density of the metal, are used widely for assigning the behavior of ancillary ligands.[66−68] However, ν_{NO} stretching frequency spans a much larger range of values and is thus an even more sensitive probe. Furthermore, coordination of nitrosyl, because of the possibility of two geometries, can also be associated with modifications in the metal coordination when a change from 18 to 16 electrons is possible. Such behavior depends on a number of factors such as the nature of the metal and all ligands. The redox properties of ruthenium make Ru(II) and Ru(0) accessible. The present study reveals that for some ligands that are not π-donors two geometries corresponding to the oxidized and reduced states are very close in energy, in contrast with experimental evidence for a single structure. Neither the use in the calculations of more realistic phosphine ligands nor the use of a method different from DFT would drastically increase the difference in energy between the two structures. Ambiguities may remain because a difference in energy of less than 5 kcal/mol is still within the uncertainty domain. An unambiguous structural elucidation is provided by correlating the calculated and experimental NO stretching frequencies. This contrasts to some extent with the usual experimental−computational vibrational frequencies relationship that is used for suggesting structures when other methods are not available. In general, the preferred structure is the one having closer agreement between calculated and experimental vibrational frequencies. This is another example where the calculations of stretching frequencies give structural information that the relative energies are not able to provide.[69]

4. Conclusions

We present several computational approaches to the characterization of the series $RuX(CO)(NO)L_2^+$ (L = $P(^tBu)_2Me$, X = NCMe, H^-, and CO) where the geometries are difficult to assign spectroscopically. First we have shown that the full theoretical characterization of these complexes cannot be achieved by the standard procedure of systematically computing their possible structures and energies on $RuX(CO)(NO)(PH_3)_2^+$ model compounds. The computational prediction of the poten-

(65) McQuarrie, D. *Statistical Mechanics*; Harper and Row: New York, 1986.

(66) Perrin, L.; Clot, E.; Eisenstein, O.; Loch, J.; Crabtree, R. H. *Inorg. Chem.* **2001**, *40*, 5806.

(67) Frenking, G.; Frölich, N. *Chem. Rev.* **2000**, *100*, 717.

(68) Abu-Hasanayn, F.; Goldman, A. S.; Krogh-Jespersen, K. *Inorg. Chem.* **1994**, *33*, 5122.

(69) Maron, L.; Perrin, L.; Eisenstein, O.; Andersen, R. A. *J. Am. Chem. Soc.* **2002**, *124*, 5614.

tial, enthalpic, and free energies for the SP and TBP $RuX(CO)(NO)(PH_3)_2^+$ (X = NCH, H^-, and CO) does not provide a clear structural assignment, the energies being very close; the most stable also differs from the experimental one, where known. Improvements in the computational level up to CCSD(T) and introduction of solvent effects do not change this picture. Consideration of the real phosphine substituents through ONIOM calculations is more significant, though energies stay quite close. These theoretical improvements always increase computational cost, and when energy differences are small, as in this case, they are hardly conclusive. Instead we have shown here that the use of the computed values of ν_{NO} on $RuX(CO)(NO)(PH_3)_2^+$ and its comparison with experimental values can be much less computer demanding and much more conclusive.

Direct comparison of computed and experimental ν_{NO} is not very informative. In a key finding, the correlation between the series of computed and experimental values of ν_{NO} is conclusive. This has allowed us to characterize $Ru(NCMe)(CO)(NO)L_2^+$ as SP and $Ru(H)(CO)(NO)L_2$ and $Ru(CO)_2(NO)L_2^+$ as TBP. Thus, the structural elucidation of $RuX(CO)(NO)L_2^+$ (X = NCH, H^-, and CO) is resolved by the correlation between the experimental and theoretical NO frequencies.

Acknowledgment. We thank Prof. Kenneth G. Caulton (Indiana) for helpful discussions. D.B. and F.M. acknowledge financial support from the Spanish MCyT (Project No. BQU2002-04110-CO2-02) and FEDER, the Catalan DURSI (Project No. 2001SGR00179), and the ICIQ Foundation.

Supporting Information Available: The potential, enthalpic, and free energies and Cartesian coordinates of the 11 Becke3LYP optimized geometries reported in the text. This material is available free of charge via the Internet at http://pubs.acs.org.

OM049536+